# Sensitivity of Glaciers in the European Alps to Anthropogenic Atmospheric Forcings: Case Study of the Argentière Glacier

Léo Clauzel, Martin Ménégoz, Adrien Gilbert, Olivier Gagliardini, Delphine Six, Guillaume Gastineau, Christian Vincent

Geophysical Research Letters

RESEARCH LETTER
10.1029/2022GL100363

# Sensitivity of Glaciers in the European Alps to Anthropogenic Atmospheric Forcings: Case Study of the Argentière Glacier

**Léo Clauzel[1], Martin Ménégoz[1], Adrien Gilbert[1], Olivier Gagliardini[1], Delphine Six[1], Guillaume Gastineau[2], and Christian Vincent[1]**

[1]CNRS, IRD, Grenoble INP, IGE, University Grenoble Alpes, Grenoble, France, [2]UMR LOCEAN, CNRS, IRD, MNHN, IPSL, Sorbonne Université, Paris, France

**Key Points:**

- Glacier simulations forced with climate model outputs are used to explore natural and anthropogenic imprints on Argentière Glacier
- Statistical downscaling needs to preserve the trends and the physical relationship between temperature and precipitation
- The anthropogenic imprint on Argentière Glacier mass emerged in 2008, 30 years after the emergence of the temperature signal

**Supporting Information:**

Supporting Information may be found in the online version of this article.

**Correspondence to:**

L. Clauzel,
leo.clauzel@univ-grenoble-alpes.fr

**Citation:**

Clauzel, L., Ménégoz, M., Gilbert, A., Gagliardini, O., Six, D., Gastineau, G., & Vincent, C. (2023). Sensitivity of glaciers in the European Alps to anthropogenic atmospheric forcings: Case study of the Argentière Glacier. *Geophysical Research Letters*, *50*, e2022GL100363. https://doi.org/10.1029/2022GL100363

Received 18 JUL 2022
Accepted 14 JUN 2023



**Abstract** This study aims to quantify the contribution of anthropogenic forcings on the retreat of the Argentière Glacier (European Alps). The glacier evolution is simulated over 1850–2014 following retrospective scenarios produced with the IPSL-CM6-LR climate model, with and without natural and anthropogenic forcings. The scenarios used to force an ice flow model are statistically downscaled, preserving the long-term trends and the physical consistency between precipitation and temperature. Since the late 19th century, the regional aerosol cooling has partially counteracted the greenhouse gas-induced warming, delaying the time of emergence of the anthropogenic signal. The anthropogenic signal emerged from natural variability in 1979 for temperature and surface melting, and in 2008 for the glacier mass, whereas its snout position in 2014 remains compatible with natural variability. From the total mass loss between 1850 and 2014, 66% [21%–111%] is attributed to anthropogenic activities.

**Plain Language Summary** This work aims to quantify the anthropogenic impact on the Argentière Glacier with respect to changes related to climate natural variability. We use a detection-attribution approach to produce retrospective ensemble simulations of the climate and the glaciers, with and without greenhouse gasses and aerosol forcings over 1850–2014. The time of emergence of the anthropogenic signal, that is, the date when it becomes statistically distinguishable from climate natural variability, occurs in 1979 for temperature in the Argentière location, with warming reaching 1.35°C in 2014 relative to 1850. The emergence of the anthropogenic signal occurs later for the glacier changes: the snout position is still compatible with natural variability in 2014, whereas for the glacier mass change, it occurred in 2008, ∼30 years after that of the temperature. In 2014, 66% [21%–111%] of the total mass loss since 1850 can be attributed to anthropogenic activities, a result that is dependent on the natural variability estimated from the climate model used in this study. The combination of increasing concentration of greenhouse gasses and decreasing aerosols in the atmosphere led to an acceleration of the glacier retreat over the last 3 decades.

## 1. Introduction

Glaciers around the world retreated dramatically over the last decades. Glacier retreat is an iconic symbol of climate change. It contributes significantly to sea level rise (Allan et al., 2021) and is also a threat to water availability, especially where glaciers play the role of freshwater reservoirs critical for biodiversity and human societies (Kaser et al., 2010; Laurent et al., 2020; Milner et al., 2017; Viani et al., 2018).

Glaciers in the Alps reached a maximum during the Little Ice Age (LIA; Holzhauser et al., 2005; Zumbuhl et al., 2008). This cold period was induced by strong volcanic activity and a minimum of solar activity, with a starting date estimated between 1250 and 1400 (Mann et al., 2009; Wanner et al., 2022). The LIA is a globally asynchronous cold event (Neukom et al., 2019) interspersed with milder periods (Hawkins et al., 2017). In Northwestern Europe, it reached a maximum during the 17th century and a last phase from 1800 to 1850 that favored large glacier extents in the Alps (Brönnimann et al., 2019).

The retreat of glaciers started during the middle of the 19th century in the Alps, simultaneously with the commencement of substantial greenhouse gas (GHG) emissions by humans. The exact causes of this retreat are still debated, since the temperature increase at the end of the 19th century was relatively small, and other factors such as decadal variability in precipitation (Schmeits & Oerlemans, 1997; Vincent et al., 2005) have likely affected glaciers. Painter et al. (2013) suggested that the deposition of aerosols on snow, by absorbing the solar radiation, contributed significantly to the glacier retreat at the end of the LIA. Sigl et al. (2018) suggested that

glacier retreat during the 19th century preceded the emergence of this aerosol forcing. Future glacier projections need to be considered carefully as the sensitivity of glaciers to external forcings and internal climate variability remains uncertain (Marzeion et al., 2020).

Detection-attribution studies, combining climate models and observations of surface air temperature, have been used to estimate the climate response to external forcings. Such studies typically estimate that the global warming of +1.2°C (±0.15°C), observed in 2010–2020 as compared to the pre-industrial era, can be decomposed into +1.5°C (±0.3°C) contribution from GHGs and −0.4°C (±0.3°C) contribution from other forcings (Eyring et al., 2021; Gillett et al., 2021; Haustein et al., 2017; Ribes et al., 2021). These other forcings include the effect of anthropogenic aerosols that cool the atmosphere. Detection-attribution methods highlight the climate response to external forcings with respect to internal variability, that is, the internal processes generating variability within the climate system independently from external forcings. Following such an approach, Roe et al. (2017, 2021) suggested that 100% of the glacier global mass loss from the pre-industrial era is explained by anthropogenic forcings. Glacier models have been successfully used to estimate the natural and anthropogenic imprints on large samples of glaciers (Hirabayashi et al., 2016; Huston et al., 2021) or on all the glaciers on Earth (e.g., Marzeion et al., 2014; Zemp & Marzeion, 2021), to quantify in particular their contribution to sea level changes (Huss & Hock, 2015; Slangen et al., 2016).

An increasing number of observational data now permits the quantification of glacier volume changes at the global scale from the 2000s onwards (Hugonnet et al., 2021). However, local observations remain insufficient to accurately simulate the volume, area and position of any specific glacier over long periods and at interannual timescales. In this study, we use a 3D ice flow model coupled to a distributed surface mass balance model that allows a detailed estimation of the glacier mass balance and snout position. This model is forced with statistically adjusted atmosphere-ocean general circulation model (AOGCMs) outputs. The adjustment is designed to reproduce the variability of the atmospheric local variables, as well as the physical consistency between them (Gutierrez et al., 2019; Latombe et al., 2018; Luo et al., 2018; Vaittinada Ayar et al., 2021).

The aim of this study is to investigate the natural and anthropogenic drivers of glaciological changes in the European Alps, using a physical approach which can be compared with larger-scale studies based on a large degree of parameterization. This study focuses on the Argentière Glacier for which a large number of observations enables an accurate model calibration. Retrospective simulations are conducted from pre-industrial conditions, that is, from 1850, a date when the anthropogenic imprint on the climate system was very low, to 2014, the end of the period covered by the historical simulations available from CMIP6 (Coupled Model Intercomparison Phase 6). This enables the quantification of the glacier response to anthropogenic forcing with respect to internal climate variability. After a presentation of the data and the methods in Section 2, the results are described in Section 3, before a discussion and a conclusion in Section 4.

## 2. Data and Methods

### 2.1. Local Observations and Climate Forcing

Located in the Mont-Blanc massif (Figure 1a), the Argentière Glacier is the second largest glacier in the French Alps, covering an area of 11.3 km$^2$ in 2019, extending over ∼10 km from 1,550 to 3,500 m a.s.l. (Six & Vincent, 2014). Stake measurements, geodetic observations and GPS survey data are available within the GLACIOCLIM observatory (https://glacioclim.osug.fr/). The bedrock topography is well known thanks to numerous radar observations (Rabatel et al., 2018; Vincent et al., 2009).

Surface air temperature and precipitation are extracted from the CMIP6 experiments produced with the IPSL-CM6A-LR AOGCM (Boucher et al., 2020). In particular, we use the Detection and Attribution Model Intercomparison Project (DAMIP, Gillett et al., 2016) simulations, which separately quantify the climate response to natural and anthropogenic external forcings. Here, we use a subset of the IPSL-CM6A-LR experiments: (a) *a 1,000-year control experiment based on constant pre-industrial forcing*; (b) a 10-member historical experiment (*hist*) that includes all natural and anthropogenic forcing changes and (c) 3 sets of 6-member experiments, including changes of only the natural (*nat*), only the anthropogenic aerosol (*aer*) and only the anthropogenic greenhouse gas (*ghg*) forcings. The *hist* simulations also include the effect of changing stratospheric ozone and land use. The first of these two forcings affecting mainly the Southern Hemisphere (Gillet & Peringer, 2012; Previdi & Polvani, 2014) and the second one being negligible in the Mont Blanc area, both of them are neglected in this

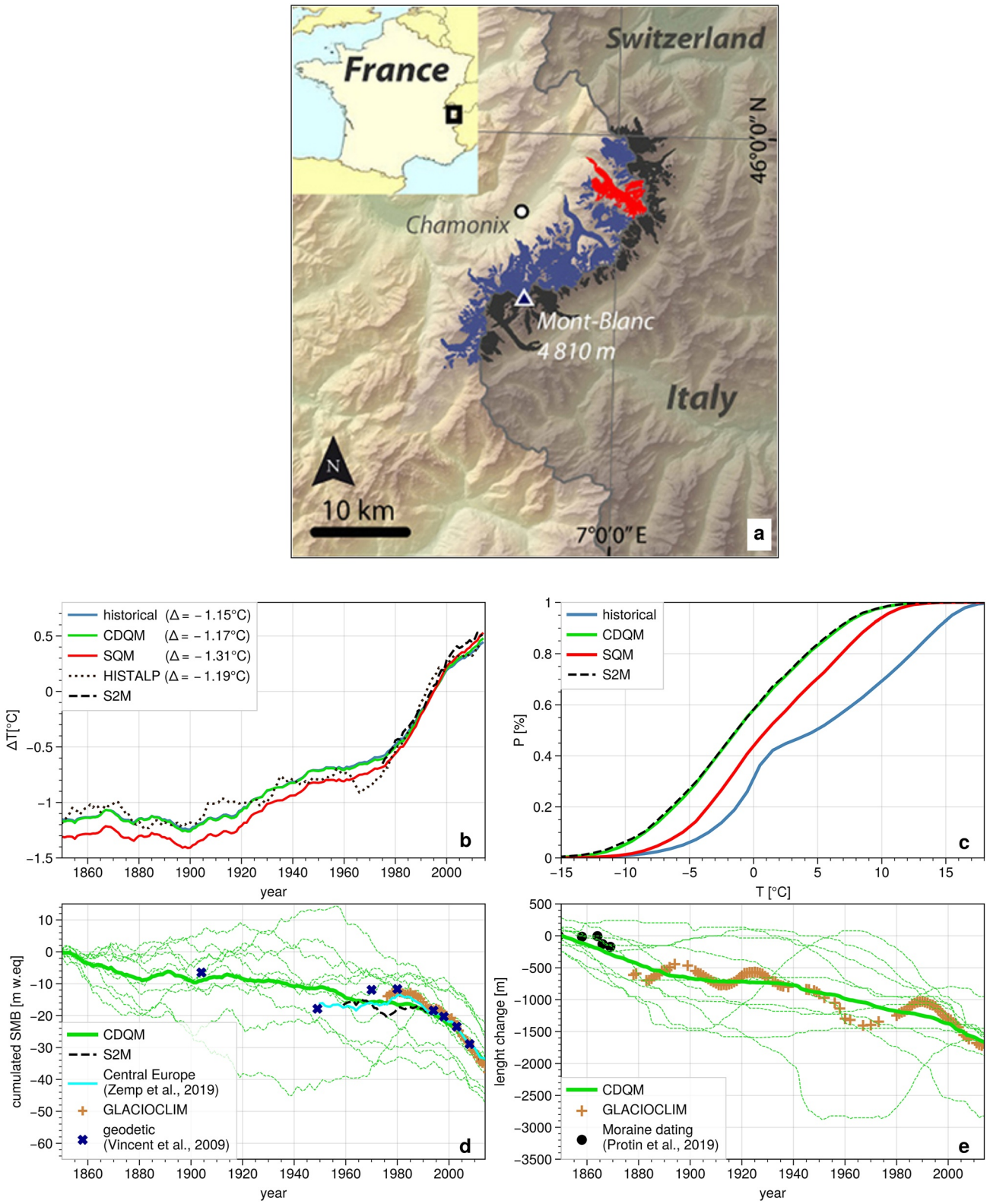


**Figure 1.**

study. The natural external forcings designate here the effects of volcanic aerosols and incoming solar radiation changes. The simulations are available over 1850–2014 and the member-experiments differ only in their initial conditions, which are sampled from the 1,000-year control experiment. Corresponding members from one experiment to another one have the same initial conditions. From the control experiment, we subsample an additional 6-member ensemble simulation defined *ctr*. The members in *ctr* are chunks of the control experiment starting from the same initial conditions as *nat*, *aer*, and *ghg*. Hereafter, we use the term "internal variability" to describe the variability sampled among the different ensemble members. The S2M reanalysis available for the different French Alpine regions with a 300 m vertical resolution (Vernay et al., 2022) is used to statistically adjust the AOGCM data extracted at the gridpoint containing the Argentière Glacier.

### 2.2. Statistical Downscaling of Climate Data

The daily AOGCM temperature and precipitation are simultaneously bias corrected and downscaled at the monthly timescale by statistically adjusting the *hist* experiment to the S2M reference at 2,400 m a.s.l., that is, close to the glacier mean elevation. The adjustment is calibrated over 1975–2014 with the 10 *hist* members and is then applied to the whole set of ensemble experiments *hist*, *nat*, *aer*, *ghg*, and *ctr*, considering a stationary correction over 1850–2014.

Temperature is adjusted with the Quantile Delta Mapping (QDM, Cannon et al., 2015), to ensure a conservation of the trend provided by the AOGCM. The 2D-variable successive conditional approach of Piani and Haerter (2012) is then followed by applying a Simple Quantile Mapping (SQM, Panofsky & Brier, 1968) for precipitation, separately for five quantiles of temperature, to keep the physical consistency between the two variables. The temperature-quantile bins are defined on 40-year moving sub-periods to avoid any impact of temperature trends on the precipitation adjustment. The combination of these two statistical adjustments is defined here as the Coupled Delta Quantile Mapping (CDQM). The CDQM method ensures a conservation of the temperature trend simulated with the AOGCM that is in accordance with the HISTALP reconstruction (Böhm et al., 2010; Figure 1b), a physical precipitation-temperature relationship consistent with the S2M reanalysis (Figure 1c) as well as realistic seasonal cycles, daily and interannual variability for these two variables (Figure S1 in Supporting Information S1). It is noteworthy to highlight that the use of SQM would lead to a spurious amplification of the long-term temperature trend (Figure 1b) and an underestimation of snow accumulation as the precipitation distribution over the temperature 1°C-width bins is shifted to warmer days in the model outputs (only 35%–45% of the precipitation occurs below 0°C in the model as compared to 60% in the S2M reference, Figure 1c).

### 2.3. Glaciological Model

The glacier response to climate forcing is simulated using a coupled surface mass balance—3D ice flow model based on the Elmer/Ice finite element code (Gagliardini et al., 2013). The model solves the Stokes equation and calculates the change in elevation according to the surface mass balance (SMB), which is calculated from the daily temperature and precipitation. Details of the glacier model and its calibration are provided in Supporting Information S1 (Text S1 and Table S1).

### 2.4. Modeling Strategy

The glacier is initialized to a steady-state geometry (stationary volume and surface elevation) matching the 1820 moraine. This is obtained by running the SMB scheme coupled to the ice flow model forced with the 1975–2015 S2M data, assuming a shift in temperature $\Delta T_0$ and unchanged precipitation rates. This method ensures to keep the seasonal and diurnal variability for which the model is calibrated. A value of $-1.30$°C for $\Delta T_0$ is required to obtain, after ∼150 years (not shown), a stationary glacier geometry, with a snout that matches the 1820 moraine. This date was chosen because the glacier was close to equilibrium with the climate over the last centuries as its

**Figure 1.** (a) Location of the Argentière Glacier (red) as well as French (blue) and Swiss (black) glaciers. (b) 30-year running mean temperature anomaly with respect to the 1975–2014 mean, averaged over members in *hist* (blue), adjusted with SQM (red) and CDQM (green), extracted from HISTALP (black dotted) and from S2M (black dashed line). Δ is the difference between the 1850–1875 and the 1975–2014 means; (c) cumulative distribution function of precipitation over 1°C-wide bins of temperature, averaged over members; (d) cumulated SMB and (e) length change from 1850 for individual members (dashed lines) and ensemble mean (solid lines) in *hist* (green) and simulated with S2M (black line). Argentière Glacier SMB estimated with GLACIOCLIM in situ data (brown crosses) and geodetic observations (blue crosses) and central european glaciers SMB estimate from Zemp and Marzeion (2021, cyan). Proxies (black points) are derived from cosmogenic surface exposure dating of moraines (Protin et al., 2019).

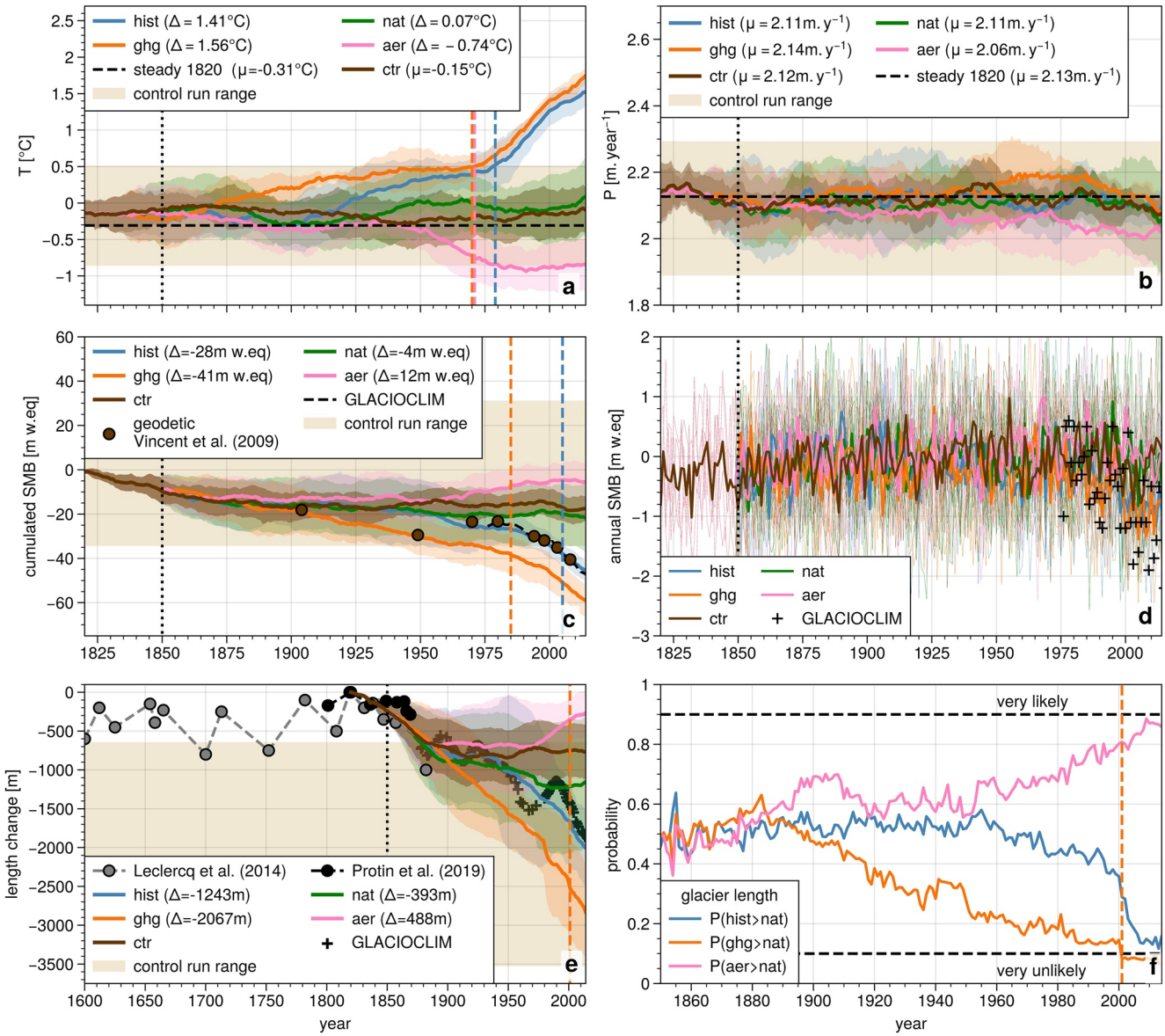


**Figure 2.** 30-year running mean of (a) adjusted temperature and (b) adjusted precipitation; (c) cumulated SMB from 1820; (d) annual SMB; (e) length change from 1820 and (f) empirical probability of having a larger glacier length than *nat* computed by comparing experiment distributions based on 1,000-time bootstrap resampling. Solid lines are 6-member means, shading corresponds to the 1-$\sigma$ member range, vertical black lines show the spin-up end. Vertical colored dashed lines indicate the year by which it is very likely or very unlikely to have a higher temperature or a lower value for SMB and glacier length than in *nat* as computed in (f). Steady 1820 in (a) and (b) refers to the climate conditions required to get the 1820 steady state. The light brown bands in (a, b, c, and e) highlight the spread (min-max) simulated in a 800 years control experiment based on constant natural forcing (a 1,000 years experiment from which a 200 years spinup is excluded). The deltas given in panels (ace) are the differences computed between the experiments with respect to *ctr* in 2014.

front did not vary significantly over 1600–1800 (Leclercq et al., 2014; Figure 2e). An additional spin-up has been produced over 1820–1850, using the 30-year periods in the control experiment that precede the initial conditions of the different members, to adjust the glacier shape to the internal climate variability specific to these members.

## 3. Results

### 3.1. Observed Versus Simulated Glacier Changes

By construction, there is a good agreement between the SMB estimated from stake observations and those simulated with the S2M data over the reference period 1975–2014 (similar means, interannual variabilities and trends,

Figure S2 in Supporting Information S1). The ensemble mean of the experiment is also close to the observed SMB. The cumulative SMB shows stabilized values during the 1970s followed by a dramatic retreat from the mid-1980s onwards reaching a cumulative change of −35m.w.eq. (Figure 1c) and a length change of −1,700 m in 2014 (Figure 1d) compared to the 1850 levels. The consistency between the model and the observations before 1975 demonstrates that the glaciological model can replicate both the SMB and the glacier flow (Figures 1d and 1e). This also confirms the realism of the adjusted AOGCMs outputs applied to the glaciological model. The large spread in the ensemble members suggests that internal climate variability can induce large low-frequency variations in glacier mass and length (Figures 1d and 1e).

### 3.2. Pre-Industrial Conditions

The experiments are spun-up from an initial steady state imposed by the 1820 moraine, which can be simulated with a temperature shift of $\Delta T_0 = -1.30$°C with respect to the 1975–2015 mean (Section 2.4). This $\Delta T_0$ is close to, albeit slightly cooler than, the adjusted AOGCM ensemble mean $\Delta T$ that reaches −1.17°C (Figure 1b). This slight temperature difference explains why there is a negative trend for SMB and glacier length during this 1820–1850 spin-up period. This corresponds to a relaxation from the LIA conditions of the glacier without any trend of temperature and precipitation (Figure 2). This is also visible in the general snout retreat for all the members in Figure 3a, with a member spread overwhelming the 1850 position that highlights the effect of internal variability on the glacier extent during this 30-year period. The large member spread in *ctr* (Figure 2e) suggests a large panel of responses of the glacier length to internal climate variability. However, the large glacier extent considered in the initial state might affect the glacier during the entire period of simulation (194 years over 1820–2014). To further understand the extreme position of the glacier during the end of the LIA, an additional 1,000-year simulation was run with the atmospheric forcing extracted from the control experiment. In this experiment, the glacier volume and extent never again reach the 1820–1850 observed levels, evidence that they cannot be explained by internal variability alone (Figure S3 in Supporting Information S1). The 30 years mean temperature reaches a minimum of −0.9°C (Figure 2a and Figure S3a in Supporting Information S1), a low value compared to the 1,000 years mean (−0.15°C). Such a cold event is however too short to induce a glacier extent reaching the moraine of 1850 (Figures S3c and S3d in Supporting Information S1). The glacier observation shows a larger extent over 1600–1850 compared to the spread of the control run (Figure 2e), highlighting a missing driver. This likely reflects the influence of natural forcings during the LIA.

### 3.3. Forced Versus Climate Internally Driven Signals

For a strict comparison with the 6-member DAMIP IPSL experiments *ghg*, *aer*, and *nat*, only the 6 corresponding members are retained in *ctr* and *hist* (Figures 2 and 3). Figure 2a highlights the local warming in *hist* that intensified in the 1980s and reached +1.41°C compared to *ctr* in 2014. This warming is mainly related to GHGs (+1.56°C) and is partly compensated by the cooling effect of anthropogenic aerosols (−0.74°C). The *nat* and *ctr* spread are almost overlaid, suggesting a negligible impact of natural forcing at the local scale over 1850–2014 (+0.07°C). Precipitation rates are stable and similar in all the experiments, suggesting a minor impact of external forcings on this variable, except in *ghg* for which precipitation is slightly strengthened and in *aer* for which precipitation is slightly decreased (Figure 2b). Although the temperature increase due to GHGs is twice as large as the decrease due to aerosols, the GHG and aerosol effects on precipitation nearly cancel each other. These changes in precipitation are related to the radiative forcing of GHGs and aerosols, potentially enhanced by atmospheric circulation changes (Myhre et al., 2017). The resulting precipitation rates remain nearly unchanged in *hist* and *nat*.

In 2014, the ensemble mean of the cumulated SMB reached −45m.weq in *hist*, an intermediate level between the aer (−5m.weq) and the ghg (−60m.weq) values (Figure 2c). The cumulated SMB reached −18 and −22m.weq in *ctr* and *nat* respectively, highlighting a relaxation from the LIA conditions in the absence of anthropogenic forcings. The interannual variability of the SMB is relatively high in both the observations and the model (Figure 2d), and positive values never occurred in the observations after 2001. According to geomorphological observations (Leclercq et al., 2014), the position of the Argentière Glacier front varied between −800 and 0 m over 1600–1820, reaching its maximum in 1820 (Figure 2e). In 2014, it was observed at −2,000 m, a retreat reproduced in *hist* which corresponds to an intermediate state between *ghg* (−2,800 m), *nat* (−1,200 m), and *aer* (−300 m).

The overlap between the ensemble experiment spreads is used to perform a signal-to-noise analysis for the different variables, by computing the time of emergence, defined as the time at which the signal of climate change

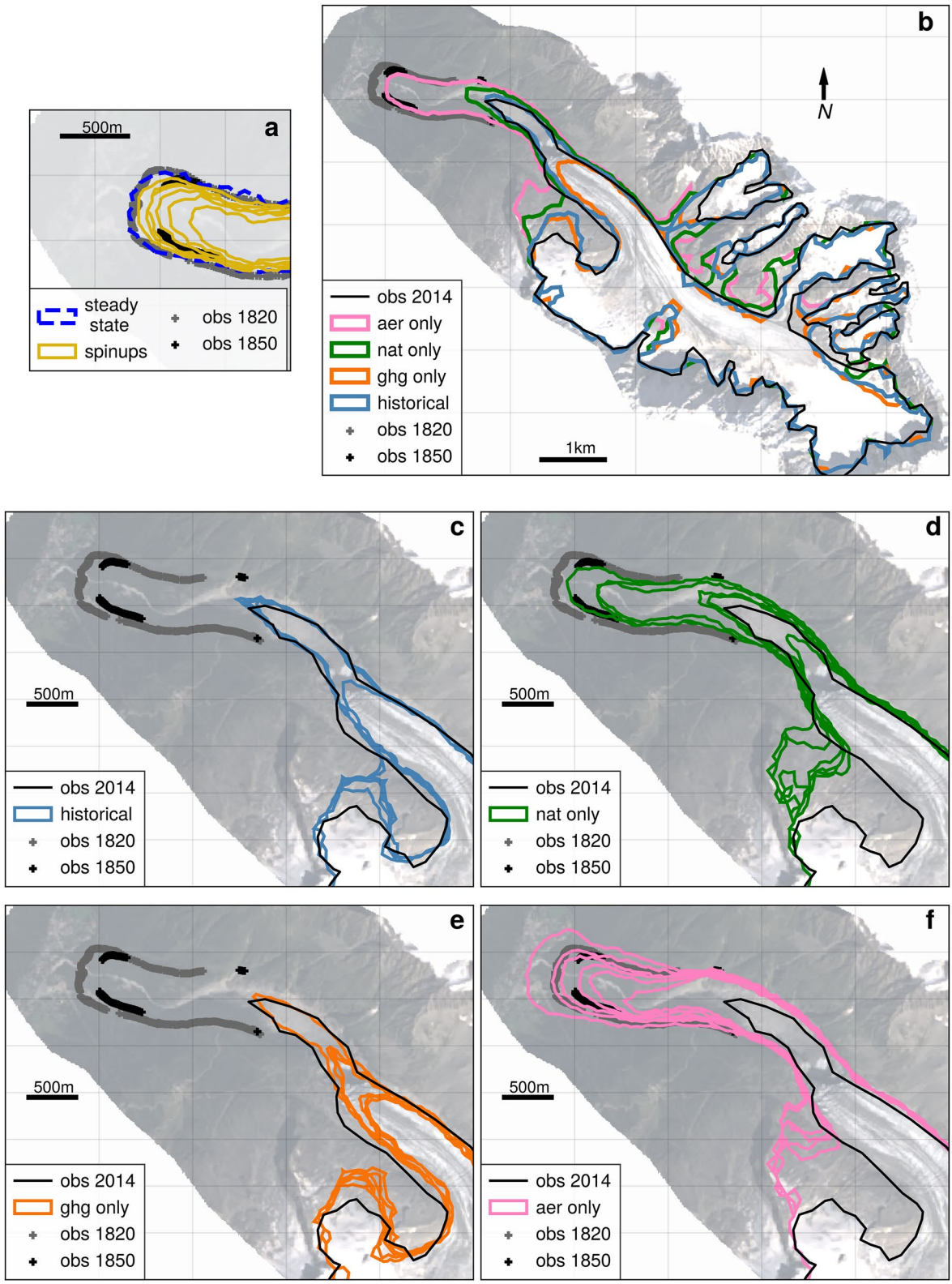


**Figure 3.** (a) Glacier extent observed in 1820 and 1850 and simulated under pre-industrial climate conditions after a 30-year spin-up experiment. (b) 6-member mean of the whole glacier area for the different experiments in 2014 and their corresponding individual members in the front area in (c) *hist*, (d) *nat*, (e) *ghg*, and (f) *aer*. The black line is the observed glacier extent in 2014 and the gray and black crosses correspond to the 1820 and 1850 moraine observations from Protin et al. (2019).

emerges from the noise of natural climate variability (Allan et al., 2021; Hawkins & Sutton, 2012). Here, following Mudelsee et al. (2014), it is estimated by calculating the probability that the glacier is larger than what is simulated in *nat* by resampling 1,000 times over the members. The vertical bars in Figures 2a, 2b, 2c, 2e, and 2f highlight the year when this probability is very unlikely ($P < 0.1$). In *ghg*, the time of emergence occurs in 2001 for the glacier length, in 1987 for SMB and in 1970 for temperature. The anthropogenic signal has not emerged significantly before 2014 for the glacier length in *hist* ($P = 0.13$), whereas it emerged in 2008 for SMB and in 1979 for temperature.

The glacier extent is shown in Figure 3b: the glacier extent simulated in *hist* is close to the 2014 observation, the retreat is less pronounced in *nat*, more pronounced in *ghg* and the glacier comes back to the LIA state in *aer*. The spatial impact of climate internal variability on the Argentière Glacier is depicted in Figures 3c–3f. Most of the *hist* members are concentrated close to the 2014 observation except one that retreated more. The *nat* ensemble shows a large spread, with members extending from the 1850 moraine to areas located at higher elevation than the 2014 observation. The entire *ghg* ensemble show extents located at higher elevation than the 2014 observation, whereas all the members of the *aer* ensemble extend around the LIA moraines.

## 4. Discussion and Conclusions

The time of emergence of anthropogenic signals in the Argentière Glacier was investigated using the adjusted IPSL-CM6 AOGCM to force an ice-flow model coupled to a SMB scheme. The effects of GHGs, anthropogenic aerosols and natural forcings are disentangled using dedicated detection-attribution AOGCM runs. The unavoidable adjustment required to bias-correct and downscale the AOGCM outputs to the local scale must be considered with caution to preserve the temperature trends from the climate model as well as the physical consistency between temperature and precipitation. Other simple statistical adjustments might result in spurious trends and erroneous accumulation rates.

The temperature change simulated with the AOGCM over 1850–2014 (1.17°C) is similar to that found in HISTALP (1.19°C) and the glacier length simulated over 1820–1850 is consistent with the moraine observations. This gives confidence in our modeling strategy, demonstrating that: (a) the extreme state of the glacier at the end of the LIA is not compatible with internal climate variability alone in our modeling framework. It is probably explained by volcanic activity and changes in solar radiation (Brönnimann et al., 2019; Mann et al., 2009), likely reinforced by snow, sea-ice and ocean feedbacks (Wanner et al., 2022). (b) A part of the retreat of the Argentière Glacier would have likely occurred without any anthropogenic forcing (−12m.weq over 1850–2014 in *nat*). When excluding anthropogenic forcing, the glacier snout is simulated at an intermediate elevation between the 1850 and 2014 positions. However, both the 1850 extent and the positions higher than those observed in 2014 are compatible with natural variability during this period, suggesting a large imprint of internal climate variability on the glacier extent. Such internal variability might be overestimated here due to the strong multidecadal internal variability simulated with IPSL-CM6-LR (Parsons et al., 2020). Nevertheless, the shape of the glacier in 2014 is still impacted by its large volume reached at the end of the LIA, an initial state that can affect the glacier extent during ∼200 years in our experimental framework. Ensemble spreads are larger in *nat* than in *hist* and *ghg*, suggesting that anthropogenic GHGs reduced the interannual to interdecadal variability of temperature and precipitation in the Alps, a hypothesis demonstrated at the global scale for the IPSL-CM6-LR model in Bonnet et al. (2021).

By comparing *hist* and *nat*, we estimate the cumulative mass loss of the Argentière Glacier due to anthropogenic forcings over 1850–2014 to be 66% [21%–111%, uncertainty in ±std]. This local estimate is lower than the global estimate of Roe et al. (2021), which ranges from 85% to 130% for valley type glaciers. However, our estimate is close to the 55% reported by Marzeion et al. (2014) for Central Europe. Using a physical approach highly constrained by observations, we assume that the uncertainty provided here is mainly the result of internal climate variability whereas global estimates generally do not disentangle internal variability from model uncertainties. The added-value of our approach relies on the possibility to physically simulate the glacier extent in different climate scenarios, a goal that cannot be achieved in global idealized studies. The similar SMB evolution of the Argentière Glacier compared to the other glaciers in the Alps during the last century (Figure 1d) and in general, the observed common climatic signal from Alpine glaciers (Davaze et al., 2020; Huss, 2012; Vincent et al., 2017), suggests that its response to anthropogenic forcings provides a general view of the glacier changes in the Alps.

Overall, the length of glaciers is an interesting proxy of the decadal to centennial climate variability because it is easy to observe and acts as a climate integrator, smoothing the high frequency variability of atmospheric forcing.

Conversely, glacier lengths show a wider range of response to internal climate variability than temperature and SMB. Indeed, the position of the front is largely influenced by the local topographic conditions such as valley shape and slope distribution. By using a 3D ice flow model, we can accurately simulate the glacier length and its dependence on complex terrain. The next step in the ice-flow model development concerns the relationship between basal sliding and subglacial hydrological processes. Including more realistic basal sliding parameterization could lead to larger spreads in the response of the glacier length to temperature changes. The increase in debris cover observed at the surface could also be taken into account in the SMB model because it could act as feedback enhancing or damping glacier changes.

The climate and glacier sensitivity to aerosol and GHG forcings might vary when they act simultaneously, because of the nonlinear processes related to local feedbacks, atmospheric circulation changes and residual internal climate variability (Deng et al., 2020). Such nonlinear response of local temperature is confirmed here. While *hist* is based on the combination of the external forcings used in *nat*, *aer*, and *ghg*, the warming found in *hist* (+1.41°C) does not reach the sum of the *aer* + *ghg* + *nat* signals with respect to *ctr* (0.07–0.74 + 1.56 = +0.89°C, Figure 2a). Similarly, the SMB changes over 1850–2014 (Figure 2c) can be decomposed in: (a) −4m.weq from natural forcings; (b) −41m.weq from GHGs; (c) +12m.weq from aerosols; with (d) a remaining trend that reflects the relaxation from the LIA conditions, reaching −8m.weq in *ctr*. Again, the sum of the SMB changes in *aer*, *ghg*, and *nat* does not reach the *hist* signal (−28m.weq) computed with respect to *ctr*. Our study provides an estimation of the glacier response to single forcings. Additional sensitivity experiments using all-forcings-except-one configurations would be required to quantify the nonlinear combination of the different forcings affecting glaciers. In addition, signal-to-noises at play are small in particular for glacier length (Figure 2e) that is widely affected by local topography and glacier hypsometry. Larger ensemble would be required to accurately quantify the single forcing signals with respect to internal variability. The large ensemble spreads simulated for SMB and glacier length reflect also the large centennial variability simulated with IPSL-CM6A-LR (Jiang et al., 2021). Further research using a multi-model DAMIP approach would allow a better estimation of the uncertainties, as climate signals, regional circulation changes and internal variability can vary from one AOGCM to another one (Parsons et al., 2020). Finally, additional model developments, including a full energy balance SMB model, are needed to take into account both the cooling effect of atmospheric aerosols and the melt increase related to the deposition of absorbing aerosols, a process known for its strong impact on the cryosphere (Reveillet et al., 2022) that has been neglected here.

## Data Availability Statement

GLACIOCLIM data is available at: https://glacioclim.osug.fr/. CMIP6 and DAMIP data are available on the Earth System Grid Federation (ESGF, https://esgf.llnl.gov/). The ice flow model is based on the open-source code Elmer/Ice available at http://elmerice.elmerfem.org/wiki/doku.php. The glacier meshing file, the glaciological model configurations, the data sets generated and analyzed and the python jupyter notebook used in the current study are available on the repository platform Zenodo at the following link: https://zenodo.org/deposit/6786833.

**Acknowledgments**
This study benefited from the IPSL simulations produced within the GENCI allocations 2016-A0030107732, 2017-R0040110492, and 2018-R0040110492, the computing and data centers ESPRI (Ensemble de Services Pour la Recherche à l'IPSL, https://mesocentre.ipsl.fr, CNRS, Sorbonne Université, École Polytechnique, CNES) and GRICAD (https://gricad.univ-grenoble-alpes.fr, UGA). This work is supported by the French ANR project SAUSSURE (ANR-18-CE01-0015-01). The authors thanks Felicity McCormack for improving the English in this manuscript.

## References

Allan, R. P., Cassou, C., Chen, D., Cherchi, A., Connors, L., Doblas-Reyes, F. J., et al. (2021). Summary for policymakers 32.

Böhm, R., Jones, P. D., Hiebl, J., Frank, D., Brunetti, M., & Maugeri, M. (2010). The early instrumental warm-bias: A solution for long central European temperature series 1760–2007. *Climatic Change*, *101*(1–2), 41–67. https://doi.org/10.1007/s10584-009-9649-4

Bonnet, R., Boucher, O., Deshayes, J., Gastineau, G., Hourdin, F., Mignot, J., et al. (2021). Presentation and evaluation of the IPSL-CM6A-LR ensemble of extended historical simulations. *Journal of Advances in Modeling Earth Systems*, *13*(9), e2021MS002565. https://doi.org/10.1029/2021MS002565

Boucher, O., Servonnat, J., Albright, A. L., Aumont, O., Balkanski, Y., Bastrikov, V., et al. (2020). Presentation and evaluation of the IPSL-CM6A-LR climate model. *Journal of Advances in Modeling Earth Systems*, *12*(7), e2019MS002010. https://doi.org/10.1029/2019MS002010

Brönnimann, S., Franke, J., Nussbaumer, S. U., Zumbühl, H. J., Steiner, D., Trachsel, M., et al. (2019). Last phase of the Little Ice Age forced by volcanic eruptions. *Nature Geoscience*, *12*(8), 650–656. https://doi.org/10.1038/s41561-019-0402-y

Cannon, A. J., Sobie, S. R., & Murdock, T. Q. (2015). Bias correction of GCM precipitation by quantile mapping: How well do methods preserve changes in quantiles and extremes? *Journal of Climate*, *28*(17), 6938–6959. https://doi.org/10.1175/JCLI-D-14-00754.1

Davaze, L., Rabatel, A., Dufour, A., Hugonnet, R., & Arnaud, Y. (2020). Region-wide annual glacier surface mass balance for the European Alps from 2000 to 2016. *Frontiers in Earth Science*, *8*, 149. https://doi.org/10.3389/feart.2020.00149

Deng, J., Dai, A., & Xu, H. (2020). Nonlinear climate responses to increasing $CO_2$ and anthropogenic aerosols simulated by CESM1. *Journal of Climate*, *33*(1), 281–301. https://doi.org/10.1175/jcli-d-19-0195.1

Eyring, V., Mishra, V., Griffith, G. P., Chen, L., Keenan, T., Turetsky, M. R., et al. (2021). Reflections and projections on a decade of climate science. *Nature Climate Change*, *11*(4), 279–285. https://doi.org/10.1038/s41558-021-01020-x

Gagliardini, O., Zwinger, T., Gillet-Chaulet, F., Durand, G., Favier, L., de Fleurian, B., et al. (2013). Capabilities and performance of Elmer/Ice, a new-generation ice sheet model. *Geoscientific Model Development*, *6*(4), 1299–1318. https://doi.org/10.5194/gmd-6-1299-2013

Gillet, F., & Peringer, A. (2012). Dynamic modelling of silvopastoral landscape structure: Scenarios for future climate and land use.

Gillett, N. P., Kirchmeier-Young, M., Ribes, A., Shiogama, H., Hegerl, G. C., Knutti, R., et al. (2021). Constraining human contributions to observed warming since the pre-industrial period. *Nature Climate Change*, *11*(3), 207–212. https://doi.org/10.1038/s41558-020-00965-9

Gillett, N. P., Shiogama, H., Funke, B., Hegerl, G., Knutti, R., Matthes, K., et al. (2016). The detection and attribution model intercomparison project (DAMIP v1.0) contribution to CMIP6. *Geoscientific Model Development*, *9*(10), 3685–3697. https://doi.org/10.5194/gmd-9-3685-2016

Gutiérrez, J. M., Maraun, D., Widmann, M., Huth, R., Hertig, E., Benestad, R., et al. (2019). An intercomparison of a large ensemble of statistical downscaling methods over Europe: Results from the VALUE perfect predictor cross-validation experiment. *International Journal of Climatology*, *39*(9), 3750–3785. https://doi.org/10.1002/joc.5462

Haustein, K., Allen, M. R., Forster, P. M., Otto, F. E. L., Mitchell, D. M., Matthews, H. D., & Frame, D. J. (2017). A real-time global warming index. *Scientific Reports*, *7*(1), 15417. https://doi.org/10.1038/s41598-017-14828-5

Hawkins, E., Ortega, P., Suckling, E., Schurer, A., Hegerl, G., Jones, P., et al. (2017). Estimating changes in global temperature since the preindustrial period. *Bulletin of the American Meteorological Society*, *98*(9), 1841–1856. https://doi.org/10.1175/BAMS-D-16-0007.1

Hawkins, E., & Sutton, R. (2012). Time of emergence of climate signals. *Geophysical Research Letters*, *39*(1), L01702. https://doi.org/10.1029/2011GL050087

Hirabayashi, Y., Nakano, K., Zhang, Y., Watanabe, S., Tanoue, M., & Kanae, S. (2016). Contributions of natural and anthropogenic radiative forcing to mass loss of Northern Hemisphere mountain glaciers and quantifying their uncertainties. *Scientific Reports*, *6*(1), 29723. https://doi.org/10.1038/srep29723

Holzhauser, H., Magny, M., & Zumbuühl, H. J. (2005). Glacier and lake-level variations in west-central Europe over the last 3500 years. *The Holocene*, *15*(6), 789–801. https://doi.org/10.1191/0959683605hl853ra

Hugonnet, R., McNabb, R., Berthier, E., Menounos, B., Nuth, C., Girod, L., et al. (2021). Accelerated global glacier mass loss in the early twenty-first century. *Nature*, *592*(7856), 726–731. https://doi.org/10.1038/s41586-021-03436-z

Huss, M. (2012). Extrapolating glacier mass balance to the mountain-range scale: The European Alps 1900–2100. *The Cryosphere*, *6*(4), 713–727. https://doi.org/10.5194/tc-6-713-2012

Huss, M., & Hock, R. (2015). A new model for global glacier change and sea-level rise. *Frontiers in Earth Science*, *3*. https://doi.org/10.3389/feart.2015.00054

Huston, A., Siler, N., Roe, G. H., Pettit, E., & Steiger, N. J. (2021). Understanding drivers of glacier-length variability over the last millennium. *The Cryosphere*, *15*(3), 1645–1662. https://doi.org/10.5194/tc-15-1645-2021

Jiang, W., Gastineau, G., & Codron, F. (2021). Multicentennial variability driven by salinity exchanges between the Atlantic and the Arctic Ocean in a coupled climate model. *Journal of Advances in Modeling Earth Systems*, *13*(3), e2020MS002366. https://doi.org/10.1029/2020MS002366

Kaser, G., Großhauser, M., & Marzeion, B. (2010). Contribution potential of glaciers to water availability in different climate regimes. *Proceedings of the National Academy of Sciences of the United States of America*, *107*(47), 20223–20227. https://doi.org/10.1073/pnas.1008162107

Latombe, G., Burke, A., Vrac, M., Levavasseur, G., Dumas, C., Kageyama, M., & Ramstein, G. (2018). Comparison of spatial downscaling methods of general circulation model results to study climate variability during the Last Glacial Maximum. *Geoscientific Model Development*, *11*(7), 2563–2579. https://doi.org/10.5194/gmd-11-2563-2018

Laurent, L., Buoncristiani, J.-F., Pohl, B., Zekollari, H., Farinotti, D., Huss, M., et al. (2020). The impact of climate change and glacier mass loss on the hydrology in the Mont-Blanc massif. *Scientific Reports*, *10*(1), 10420. https://doi.org/10.1038/s41598-020-67379-7

Leclercq, P. W., Oerlemans, J., Basagic, H. J., Bushueva, I., Cook, A. J., & Le Bris, R. (2014). A data set of worldwide glacier length fluctuations. *The Cryosphere*, *8*(2), 659–672. https://doi.org/10.5194/tc-8-659-2014

Luo, M., Liu, T., Meng, F., Duan, Y., Frankl, A., Bao, A., & De Maeyer, P. (2018). Comparing bias correction methods used in downscaling precipitation and temperature from regional climate models: A case study from the Kaidu River Basin in Western China. *Water*, *10*(8), 1046. https://doi.org/10.3390/w10081046

Mann, M. E., Zhang, Z., Rutherford, S., Bradley, R. S., Hughes, M. K., Shindell, D., et al. (2009). Global signatures and dynamical origins of the Little Ice Age and Medieval Climate Anomaly. *Science*, *326*(5957), 1256–1260. https://doi.org/10.1126/science.1177303

Marzeion, B., Cogley, J. G., Richter, K., & Parkes, D. (2014). Attribution of global glacier mass loss to anthropogenic and natural causes. *Science*, *345*(6199), 919–921. https://doi.org/10.1126/science.1254702

Marzeion, B., Hock, R., Anderson, B., Bliss, A., Champollion, N., Fujita, K., et al. (2020). Partitioning the uncertainty of ensemble projections of global glacier mass change. *Earth's Future*, *8*(7), e2019EF001470. https://doi.org/10.1029/2019EF001470

Milner, A. M., Khamis, K., Battin, T. J., Brittain, J. E., Barrand, N. E., Füreder, L., et al. (2017). Glacier shrinkage driving global changes in downstream systems. *Proceedings of the National Academy of Sciences of the United States of America*, *114*(37), 9770–9778. https://doi.org/10.1073/pnas.1619807114

Mudelsee, M., Bickert, T., Lear, C. H., & Lohmann, G. (2014). Cenozoic climate changes: A review based on time series analysis of marine benthic $\delta^{18}O$ records. *Reviews of Geophysics*, *52*(3), 333–374. https://doi.org/10.1002/2013RG000440

Myhre, G., Forster, P. M., Samset, B. H., Hodnebrog, Ø., Sillmann, J., Aalbergsjø, S. G., et al. (2017). PDRMIP: A precipitation driver and response model intercomparison project—Protocol and preliminary results. *Bulletin of the American Meteorological Society*, *98*(6), 1185–1198. https://doi.org/10.1175/BAMS-D-16-0019.1

Neukom, R., Steiger, N., Gómez-Navarro, J. J., Wang, J., & Werner, J. P. (2019). No evidence for globally coherent warm and cold periods over the preindustrial Common Era. *Nature*, *571*(7766), 550–554. https://doi.org/10.1038/s41586-019-1401-2

Painter, T. H., Flanner, M. G., Kaser, G., Marzeion, B., VanCuren, R. A., & Abdalati, W. (2013). End of the Little Ice Age in the Alps forced by industrial black carbon. *Proceedings of the National Academy of Sciences of the United States of America*, *110*(38), 15216–15221. https://doi.org/10.1073/pnas.1302570110

Panofsky, H. A., & Brier, G. W. (1968). *Some applications of statistics to meteorology*. Earth and Mineral Sciences Continuing Education, College of Earth and Mineral Sciences.

Parsons, L. A., Brennan, M. K., Wills, R. C. J., & Proistosescu, C. (2020). Magnitudes and spatial patterns of interdecadal temperature variability in CMIP6. *Geophysical Research Letters*, *47*(7), e2019GL086588. https://doi.org/10.1029/2019GL086588

Piani, C., & Haerter, J. O. (2012). Two dimensional bias correction of temperature and precipitation copulas in climate models. *Geophysical Research Letters*, *39*(20), L20401. https://doi.org/10.1029/2012GL053839

Previdi, M., & Polvani, L. M. (2014). Climate system response to stratospheric ozone depletion and recovery. *Quarterly Journal of the Royal Meteorological Society*, *140*(685), 2401–2419. https://doi.org/10.1002/qj.2330

Protin, M., Schimmelpfennig, I., Mugnier, J.-L., Ravanel, L., Le Roy, M., Deline, P., et al. (2019). Climatic reconstruction for the Younger Dryas/Early Holocene transition and the Little Ice Age based on paleo-extents of Argentière Glacier (French Alps). *Quaternary Science Reviews*, *221*, 105863. https://doi.org/10.1016/j.quascirev.2019.105863

Rabatel, A., Sanchez, O., Vincent, C., & Six, D. (2018). Estimation of glacier thickness from surface mass balance and ice flow velocities: A case study on Argentière Glacier, France. *Frontiers in Earth Science*, *6*. https://doi.org/10.3389/feart.2018.00112

Réveillet, M., Dumont, M., Gascoin, S., Lafaysse, M., Nabat, P., Ribes, A., et al. (2022). Black carbon and dust alter the response of mountain snow cover under climate change. *Nature Communications*, *13*(1), 1–12. https://doi.org/10.1038/s41467-022-32501-y

Ribes, A., Qasmi, S., & Gillett, N. (2021). Updated attribution of GSAT changes and implications EGU21-16112. https://doi.org/10.5194/egusphere-egu21-16112

Roe, G. H., Baker, M. B., & Herla, F. (2017). Centennial glacier retreat as categorical evidence of regional climate change. *Nature Geoscience*, *10*(2), 95–99. https://doi.org/10.1038/ngeo2863

Roe, G. H., Christian, J. E., & Marzeion, B. (2021). On the attribution of industrial-era glacier mass loss to anthropogenic climate change. *The Cryosphere*, *15*(4), 1889–1905. https://doi.org/10.5194/tc-15-1889-2021

Schmeits, M. J., & Oerlemans, J. (1997). Simulation of the historical variations in length of Unterer Grindelwaldgletscher, Switzerland. *Journal of Glaciology*, *43*(143), 152–164. https://doi.org/10.3189/s0022143000002914

Sigl, M., Abram, N. J., Gabrieli, J., Jenk, T. M., Osmont, D., & Schwikowski, M. (2018). 19th century glacier retreat in the Alps preceded the emergence of industrial black carbon deposition on high-alpine glaciers. *The Cryosphere*, *12*(10), 3311–3331. https://doi.org/10.5194/tc-12-3311-2018

Six, D., & Vincent, C. (2014). Sensitivity of mass balance and equilibrium-line altitude to climate change in the French Alps. *Journal of Glaciology*, *60*(223), 867–878. https://doi.org/10.3189/2014JoG14J014

Slangen, A. B. A., Church, J. A., Agosta, C., Fettweis, X., Marzeion, B., & Richter, K. (2016). Anthropogenic forcing dominates global mean sea-level rise since 1970. *Nature Climate Change*, *6*(7), 701–705. https://doi.org/10.1038/nclimate2991

Vaittinada Ayar, P., Vrac, M., & Mailhot, A. (2021). Ensemble bias correction of climate simulations: Preserving internal variability. *Scientific Reports*, *11*(1), 3098. https://doi.org/10.1038/s41598-021-82715-1

Vernay, M., Lafaysse, M., Monteiro, D., Hagenmuller, P., Nheili, R., Samacoïts, R., et al. (2022). The S2M meteorological and snow cover reanalysis over the French mountainous areas: Description and evaluation (1958–2021). *Earth System Science Data*, *14*(4), 1707–1733. https://doi.org/10.5194/essd-14-1707-2022

Viani, A., Condom, T., Vincent, C., Rabatel, A., Bacchi, B., Sicart, J., et al. (2018). Glacier-wide summer surface mass-balance calculation: Hydrological balance applied to the Argentière and Mer de Glace drainage basins (Mont Blanc). *Journal of Glaciology*, *64*(243), 119–131. https://doi.org/10.1017/jog.2018.7

Vincent, C., Fischer, A., Mayer, C., Bauder, A., Galos, S. P., Funk, M., et al. (2017). Common climatic signal from glaciers in the European Alps over the last 50 years. *Geophysical Research Letters*, *44*(3), 1376–1383. https://doi.org/10.1002/2016GL072094

Vincent, C., Le Meur, E., Six, D., & Funk, M. (2005). Solving the paradox of the end of the Little Ice Age in the Alps. *Geophysical Research Letters*, *32*(9), L09706. https://doi.org/10.1029/2005GL022552

Vincent, C., Soruco, A., Six, D., & Meur, E. L. (2009). Glacier thickening and decay analysis from 50 years of glaciological observations performed on Glacier d'Argentière, Mont Blanc area, France. *Annals of Glaciology*, *50*, 73–79. https://doi.org/10.3189/172756409787769500

Wanner, H., Pfister, C., & Neukom, R. (2022). The variable European little ice age. *Quaternary Science Reviews*, *287*, 107531. https://doi.org/10.1016/j.quascirev.2022.107531

Zemp, M., & Marzeion, B. (2021). Dwindling relevance of large volcanic eruptions for global glacier changes in the Anthropocene. *Geophysical Research Letters*, *48*(14), e2021GL092964. https://doi.org/10.1029/2021gl092964

Zumbühl, H. J., Steiner, D., & Nussbaumer, S. U. (2008). 19th century glacier representations and fluctuations in the central and western European Alps: An interdisciplinary approach. *Global and Planetary Change*, *60*(1–2), 42–57. https://doi.org/10.1016/j.gloplacha.2006.08.005

## References From the Supporting Information

Cuffey, K. M., & Paterson, W. S. B. (2010). *The physics of glaciers*. Academic Press.

Gilbert, A., Sinisalo, A., Gurung, T. R., Fujita, K., Maharjan, S. B., Sherpa, T. C., & Fukuda, T. (2020). The influence of water percolation through crevasses on the thermal regime of a Himalayan mountain glacier. *The Cryosphere*, *14*(4), 1273–1288. https://doi.org/10.5194/tc-14-1273-2020

Gimbert, F., Gilbert, A., Gagliardini, O., Vincent, C., & Moreau, L. (2021). Do existing theories explain seasonal to multi-decadal changes in glacier basal sliding speed? *Geophysical Research Letters*, *48*(15), e2021GL092858. https://doi.org/10.1029/2021GL092858

Hock, R. (1999). A distributed temperature-index ice- and snowmelt model including potential direct solar radiation. *Journal of Glaciology*, *45*(149), 101–111. https://doi.org/10.3189/S0022143000003087

Oerlemans, J. (2001). *Glaciers and climate change*. CRC Press.

Weertman, J. (1957). On the sliding of glaciers. *Journal of Glaciology*, *3*(21), 33–38. https://doi.org/10.3189/S0022143000024709